

Fine Manipulation and Dynamic Interaction in Haptic Teleoperation

Carlo Tiseo[†], Quentin Rouxel[†], Zhibin Li, and Michael Mistry

Abstract—The teleoperation of robots enables remote intervention in distant and dangerous tasks without putting the operator in harm’s way. However, remote operation faces fundamental challenges due to limits in communication delays. The proposed work improves the performances of teleoperation architecture based on Fractal Impedance Controller (FIC) by integrating into the haptic teleoperation pipeline a postural optimisation that also accounts for the replica robots’ physical limitations. This update improves dynamic interactions by trading off tracking accuracy to maintain the system within its power limits. Thus, allowing fine manipulation without renouncing the robustness of the FIC controller. Additionally, the proposed method allows an online trade-off between tracking the autonomous trajectory and executing the teleoperated command, allowing their safe superimposition. The validated experimental results show that the proposed method is robust to increased communication delays. Moreover, we demonstrated that the remote teleoperated robot remains stable and safe to interact with, even when the communication with the master side is abruptly interrupted.

I. INTRODUCTION

Teleoperation finds application in medical, space and industrial robotics. It allows remote intervention, which can be helpful to reduce the time required to complete a task, keep operators away from a dangerous situation, and enable the accessibility to a service that would be otherwise prohibitive [1]–[3]. For example, the teleoperated system can provide assistance and medical treatment remotely, allowing patients to access specialised medical operators that would be otherwise impossible to intervene. Addressing all these applications requires a modular adaptive control architecture, which is capable of fine manipulation, dynamic interaction, and robust and safe to operate even when there is a loss of connection between the master and the replica device.

Over the last few decades, there has been a steep increase in performances in teleoperated systems. Commercial devices targeting medical, military and civil applications are now available; however, their manipulation capabilities are often limited or constrained to specific types of interactions [4]–[7]. Furthermore, these systems usually require extensive tuning to be re-purposed for new applications, limiting the applicability of these systems in complex tasks that might

need, for example combining fine manipulation and dexterous dynamic interaction in an unstructured environment [1], [8], [9]. These problems are also amplified when dealing with haptic teleoperation, introducing additional complexity into the control architecture that might become more fragile to delays between the two systems [10]–[12].

A few recently proposed architectures have shown the capabilities of passive controllers in performing haptic teleoperation and manipulation in an unstructured environment [13], [14]. Passivity can be either an inherent property of the controller, or a controller can be made passive using an energy-tank [15]–[17]. Tank-based methods are limited by the presence of residual energy in the tank; therefore, the controller performance are compromised in the occurrence that the tank runs out of energy. Furthermore, the approach proposed in [17] for multi-arm teleoperation requires all the master and replica systems involved to share the same energy reservoir, which increases the computational complexity of the architecture and couples the stability of the robots’ controllers.

On the other hand, the methods proposed in [13] and [14] are based on an intrinsically passive controller, exploiting the stability proprieties of the Fractal Impedance Controller (FIC) theoretically proved in [15], [18]. Their performances show that these FIC-based methods can exploit highly non-linear stiffness profiles to generate regions of compliant behaviour without compromising the robot tracking accuracy even in the presence of communication delays. The FIC also allows to decouple the stability of the different robots and can be tuned online [13], [14]. Thus, the system can adapt online to different tasks’ requirements, perform autonomous haptic exploration and mimic human behaviour during dynamic interaction [19]–[21]. Some of the task that have been tested are driving a pile into sand, pushing a ball across a highly irregular terrain, drilling hole patterns on different materials, and cooperating with a human during unstructured tasks [13], [14]. More recently, [19] proposed an FIC-based architecture capable of mimicking human movements in dexterous tasks such as drawing and writing under uncertain interaction.

In summary, FIC architectures have shown that this controller renders the robot capable of dexterous robust interaction. Earlier architectures have been tested with feedback delays up to 1 s and controller bandwidth as low as 10 Hz both in manipulation and teleoperation [13], [15]. Previous FIC architectures have also shown that switching between teleoperation and manipulation is possible without any tuning. However, they required restarting the system to change the controller modality; there was no postural optimisation. The controller was only able to follow discrete sequences via

[†] The authors contributed equally to this paper.

This work has been supported by EPSRC UK RAI Hub ORCA (EP/R026173/1), the Future AI and Robotics for Space (EP/R026092/1), National Centre for Nuclear Robotics (NCNR EP/R02572X/1) and THING project in the EU Horizon 2020 (ICT-2017-1).

Carlo Tiseo is with the School of Engineering and Informatics, University of Sussex (Chichester 1 Room 002, Brighton BN1 9QJ, UK). All the authors are with the ECR, IPAB, School of Informatics, University of Edinburgh (10 Crichton St, Edinburgh, EH8 9AB, UK). c.tiseo@sussex.ac.uk, quentin.rouxel@ed.ac.uk

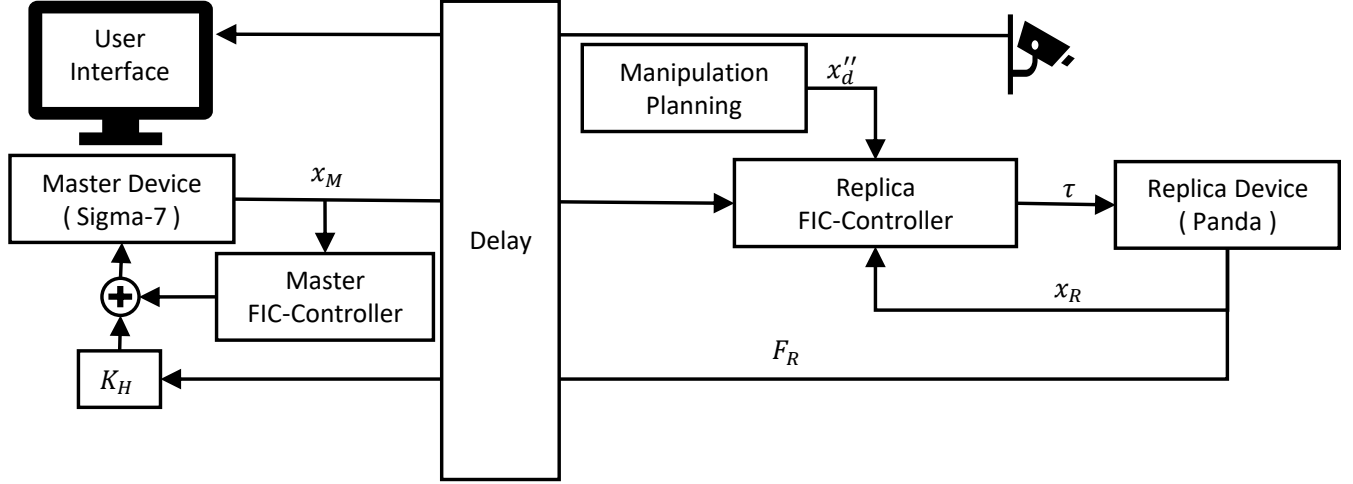


Fig. 1. User receives visual feedback from two fixed cameras pointing at the workspace and haptic feedback from the master device. Haptic force feedback produced by the Master combines the force at the Replica end effector scaled by a factor K_H , and the master FIC controller providing force feedback about the workspace boundaries determined by the Replica FIC-Controller. On the Replica side, the desired position of the manipulation planning (x_d) is combined with the user input (x_M') to generate the torque command (τ) sent to the Replica.

points and not trajectories, and it could trigger the protection mechanisms (i.e., velocity limits and torque rate) of the robot when there was a sudden acceleration due to the lack of constraints on the controller power limits. In this manuscript, we refine and integrate our earlier methods into a single architecture (Fig. 1). This new controller addresses the following points:

- 1) The proposed architecture increases the system remains operational during delayed haptic teleoperation by autonomously adjusting the robot behaviour to maintain the control commands within the system physical constraints and avoid triggering the robot protection mechanisms (i.e., velocity limits and torque rate) by trading off its tracking performance. The system has been tested for communication delays of about 200 ms, implying a feedback latency of 400 ms.
- 2) Validation that the updated replica controller on the robot allows the superimposition of teleoperated behaviour and autonomous motion by adding together these two motion components without affecting the system stability.

The control architecture is presented in section II. The experimental validation is described in section III, and they are discussed in section IV.

II. CONTROL ARCHITECTURE

The architecture in Fig. 1 has a hierarchical structure of semi-autonomous controllers, which allow controlling the replica device. The master device is used to measure the operator's movements while providing online adjustable haptic feedback. The replica controller is composed of two parallel FIC-based control that take as input the output of the manipulation planner superimposed to the position offset

recorded on the master device. Additionally, the teleoperation controller also has a velocity-based command, enabling to move the equilibrium position of the replica controller to re-centre the system workspace manually. The operator can switch between the offset and the velocity based teleoperation using a keyboard command.

A. Monodimensional Fractal Impedance Controller

The task-space control uses the FIC formulation using the force profile introduced in [22], and later redefined in [21], which is defined as follows for each dimension:

$$F_c(\tilde{x}) = \begin{cases} K_0 \tilde{x}, & \|\tilde{x}\| \leq \xi \tilde{x}_b \\ \frac{\Delta F}{2} \left(\tanh \left(\frac{\tilde{x} - \tilde{x}_b}{S \tilde{x}_b} + \pi \right) + 1 \right) + F_0, & \text{else.} \end{cases} \quad (1)$$

K_0 is the constant stiffness, $\tilde{x} = x_d - x$ is the end-effector position error, and \tilde{x}_b is the tracking error when the force saturation occurs. Being F_{\max} the saturation of the force of the controller, $\Delta F = F_{\max} - F_0$, $F_0 = \xi K_0 \tilde{x}_b$, $S = (1 - \xi) (\tilde{x}_b / (2\pi))$ controls the saturation speed, and $\xi \in [0, 1]$ control the starting of the saturation behaviour while approaching x_b . The F_c is then substituted in the attractor formulation.

$$FIC(\tilde{x}) = \begin{cases} F_c(\tilde{x}), & \text{D} \\ \frac{2F_c(\tilde{x}_{\max})}{\tilde{x}_{\max}} \left(\tilde{x} - \frac{\tilde{x}_{\max}}{2} \right), & \text{C,} \end{cases} \quad (2)$$

where (D) indicates the divergence phase, and (C) indicates the convergence phase, as defined in [15]. \tilde{x}_{\max} is the maximum state error recorded at the beginning of the last convergence phase. The convergence phase is identified using

the following conditions on the system state: $\|\tilde{x}(t)\| < \|\tilde{x}(t-1)\|$ and $\text{sign}(\tilde{x}(t)) \neq \text{sign}(\tilde{x}(t-1))$.

The FIC is an intrinsically stable controller being the algorithmic implementation of a passive non-linear oscillator with autonomous harmonic trajectories converging to the desired state [15], [20], [21]. Its autonomous trajectories also upper bound the energy and the power that the controller releases, which can be experimentally calibrated to the system to guarantee stability [15], [18]. Another benefit of this controller is that its observer coincides with its non-linear spring. This implies that being conservative, it is path independent and robust to low controller bandwidth, and feedback delays [13], [15]. Additionally, passive and conservative systems can be superimposed without affecting their stability [13], allowing to decouple the stability of the master and the replica robots in the proposed architecture.

The sole requirement to guarantee the stability of the FIC is that the used force profile is continuous with bounded derivatives (i.e., Lipschitz function) as shown in the Lyapunov stability analyses presented in [15], [18]. The proposed force profile in Eq. (1) is a smooth continuous function, which satisfies the stability condition of the FIC controllers.

B. Master Controller

The master controller also refines the earlier formulations presented in [15] and [13]. The first difference is switching to the FIC algorithm introduced in [18], [20], which removes the jump in force when switching from divergence to convergence. The second is giving the operator a direct control on the haptic feedback scaling factor (K_H). This function was implemented using the grasp degrees of freedom of the Sigma-7 as an analogue input. The online tuning of the haptic feedback is required to modulate the system responsiveness to the external interactions. Due to unbalanced inertia between the master and replica device, the interaction efforts measured on the replica will generate a higher twist on the master than the latter. This can be addressed by introducing a fixed scaling factor on the recorded forces. However, this approach also renders small interaction forces, which might be informative for some tasks, undetectable to the user interacting with the master. Therefore, we opted for online tuning of the scaling (using the grasp-dof of the Sigma-7) to enable the user to have an online control of the system responsiveness.

The operator commands the task space motion with respect to a reference equilibrium position \mathbf{x}_{Md} defined as the local origin $\mathbf{x}_{Md} = \mathbf{0}$.

$$\mathbf{f} = \text{FIC}(-\mathbf{x}_M) + K_H \mathbf{F}_R, \quad (3)$$

where \mathbf{f} is the end-effector control effort of the master device, \mathbf{x}_M is the end-effector pose of the master device. $K_H \in [0, 1]$ is the haptic gain controlled online by the user with the grasp-DoF of the Sigma-7 device. \mathbf{F}_R is the force measured at the end-effector of the replica.

The operator can choose between two control modalities for teleoperating the replica robot, which alter the interpre-

tation of the signal \mathbf{x}_M by the Replica FIC-Controller (Fig. 1). The Offset-Based Teleoperation ($\mathbf{x}'_d = \mathbf{x}_M$) gives better dexterity, but it is limited to the workspace determined by the Master range of motion. The second modality is a Velocity-Based Teleoperation ($\mathbf{x}'_d(t) = \mathbf{x}'_d(t - \Delta t) + \mathbf{x}_M \Delta t$), which allows a broader range of motion, sacrificing some dexterity.

C. Trajectory Planning for Manipulation

The trajectory planning exploits the FIC architecture presented in [19], which improves our earlier results presented in [21]–[23]. The main difference of the updated formulation is the ability to track trajectories and not only discrete sequences of via points.

The formulation used for the planner is:

$$\begin{aligned} \mathbf{x}''_d &= \int_0^t \dot{\mathbf{x}}''_d dt \\ \dot{\mathbf{x}}''_d &= \int_0^t \ddot{\mathbf{x}}''_d dt \in [-v_d, v_d] \\ \ddot{\mathbf{x}}''_d &= \begin{cases} \text{sign}(\tilde{\mathbf{x}}_t) \min(\omega_n^2 \|\tilde{\mathbf{x}}_t\|, \|\mathbf{a}_{\max}\|) - \mu \dot{\mathbf{x}}''_d, & \text{D} \\ \frac{2A_{\max}}{\tilde{\mathbf{x}}_{T0}} \left(\mathbf{x}''_d(t-1) - \frac{\tilde{\mathbf{x}}_{T0}}{2} \right) - \mu \dot{\mathbf{x}}''_d, & \text{C}, \end{cases} \end{aligned} \quad (4)$$

where $\tilde{\mathbf{x}}_t(t) = \mathbf{x}_t(t) - \mathbf{x}''_d(t-1)$, $\mathbf{x}_t(t)$ is the next point in the desired trajectory, ω_n is the desired natural frequency of the planner in rad s^{-1} , and $\mu = 0.01\omega_n$ is the viscosity. In regards of the equation for the (C) phase, A_{\max} is the acceleration associated with the maximum displacement ($\tilde{\mathbf{x}}_{T0}$) reached in the previous (D) phase. \mathbf{a}_{\max} describes the maximum acceleration limit of the movement and it is derived from the desired tangential velocity v_d as follows:

$$v_{\max} = v_p \min(v_d, \omega_n \|\mathbf{d}\|), \quad \mathbf{a}_{\max} = 2\mathbf{d} \left(\frac{v_{\max}}{\|\mathbf{d}\|} \right)^2, \quad (5)$$

where $v_p = 1.595$, \mathbf{d} is the distance vector from \mathbf{x}_t when the new command is issued.

D. Replica Controller

The torque control signal for the Replica robot is:

$$\boldsymbol{\tau} = \mathbf{C}(\mathbf{q}, \dot{\mathbf{q}}) + \mathbf{G}(\mathbf{q}) + \mathbf{J}(\mathbf{q})^T (\text{FIC}(\tilde{\mathbf{x}}_R)), \quad (6)$$

where $\mathbf{C}(\mathbf{q}, \dot{\mathbf{q}})$ and $\mathbf{G}(\mathbf{q})$ are the vectors of centrifugal, Coriolis and gravitational forces in joint space, $\mathbf{J}(\mathbf{q})$ is the kinematic Jacobian of the end-effector, and $\tilde{\mathbf{x}}_R = \mathbf{x}_d - \mathbf{x}_R$ is the tracking error of the replica robot. $\mathbf{x}_d = \mathbf{x}'_d + \mathbf{x}''_d$ and \mathbf{x}_R are the desired and measured respectively position the end-effector.

III. EXPERIMENTAL VALIDATION

The proposed method has been tested in the two experiments shown in Fig. 2 to evaluate the robustness of interaction and accuracy, which have been designed to validate the controller in ideal conditions (i.e., expert operator). The first experiment involved teleoperating the robot via

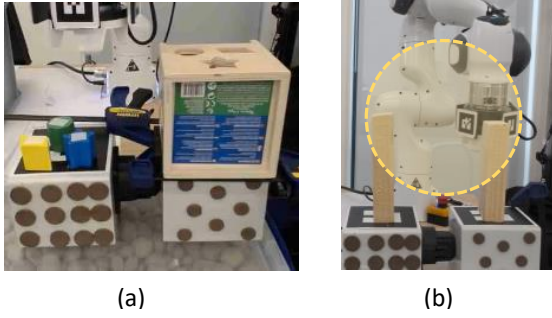


Fig. 2. Experimental Tasks: (a) Shape sorting cube experiments involving a parallelepiped, an octagonal prism, and a star-shaped dodecagonal prism. (b) Manipulator tracks the circular trajectories in yellow, and the user teleoperates the manipulator to avoid or induce interaction with the two wood obstacles.

the haptic interface to solve a shape sorting cube. For the second experiment, the manipulator is autonomously tracking a circular trajectory on a collision course with two obstacles, and the operator task is to avoid collisions between the robot and the two objects. We conducted these experiments with (one-way) communication delays of about 200 ms between the master and the replica robot, which we consider is enough to prevent the use of a haptic teleoperation without the introduction of shared autonomy algorithms in replica robots. Furthermore, the stability of the architecture was tested in the event of a loss of communication between the master and the slave robot. The FIC parameters used for the replica are $\tilde{x}_b = 0.05$ m, $K_0 = 200$ Nm⁻¹, which implies that an error up to 0.05 m is an acceptable tracking accuracy. It is worth noting that the controller can be made stiffer if needed as shown in [19].

A. The Shape Sorting Cube

The shape sorting cube is a child game training hand-eye coordination, fine motor and problem-solving skills. Consequently, this game is well suited to test the capability of the teleoperation setup of executing fine motor skills, which is also challenged by receiving limited visual feedback from only two cameras with a fixed point of view. Additionally, the experiment is designed to evaluate the architecture robustness to dynamic and unstructured interactions and its capability to pass from a force-based task to a fine motor skill without re-tuning the controller. This test is achieved by replacing the gripper with a Velcro strap attached to a static end-effector plate. These fastening tapes are constituted by two different tapes locking on each other. One of the tapes has semi-rigid hooks; the other tape has a soft pile of synthetic fabric. The degree of interlocking between the two sides determines the bonding strength. Thus, generating an inconsistent bound that is perfect for testing our controller's robustness and dynamic properties. In summary, the assigned task is: *i*) Pick up one of the objects. *ii*) Align and insert in the proper shape in the box. *iii*) Lock the object against the hole geometry and pull. *iv*) Break the Velcro strap bond and complete the task.

The dynamic characteristics of the proposed method are highlighted in the experiments' video [24]. Fig. 3 shows

the trajectory during the first shape sorting experiment. The tracking error is within the selected accuracy when the environmental interaction does not impede it. The force data also highlight how the controller can safely absorb interaction force that exceeds the maximum value that can be generated by the controller, highlighting the dynamically challenging environment generated by the selected experiment. The interaction forces recorded during the other 3 trials are shown in Fig. 4, including an experiment that includes with a loss of communication between the master and the replica. Such events generate instability in all the teleoperation architectures that require observability of both master and replica states to guarantee the stability of interaction [17]. The interaction forces recorded reach magnitudes consistently exceeding 10 N with a maximum value of 30.4 N.

Fig. 5 shows a sequence of frames extracted from the video recorded during the experiments, highlighting the four sub-tasks of this experiment. The experiment was also repeated multiple times to evaluate the robustness and repeatability. Our operator was successful in all four trials showing that the proposed method is robust and has repeatable results. The stability of a communication disconnection between master and replica robot was also successfully tested in one of these tests, validating the robustness and safety of the proposed architectures to an eventual disconnection. It is worth noting that the oscillatory behaviour shown in some of the videos after dropping the cube into the box is not an indication of instability. These motions are caused by releasing the energy accumulated in the non-linear controller spring. They are due to the error between the current pose and the desired pose required to break the bond between object and end-effector. In other words, it is like if we are pulling something with all our strength and suddenly gives up, generating an oscillation of our limbs to release the accumulated energy safely.

B. Superimposition of Manipulation and Teleoperation

One of the most challenging tasks for the operator during teleoperation is to move the end-effector across long distances accurately. To solve this issue, we have introduced the possibility of updating the end-effector pose via keyboard inputs in [14]. This solution allows for repositioning the robot workspace bypassing the haptic interface, and it works well in controlled workspaces. However, it struggles in dynamic scenarios where moving obstacles could interfere with the task. Thus, we thought that we could combine the motion reliability of a pre-planned trajectory with the flexibility of the operator's control by allowing to superimpose to a predefined motion a teleoperation command from the user. To test the feasibility of this application, we set the robot on a circular trajectory on a collision course with two obstacles. Then, the user had to teleoperate the system to avoid colliding with the two objects and try simple manipulation of the obstacles before allowing the robot to hit them.

Two trials are conducted for this experiment. The data from the first trial are shown in Fig. 7. They indicate that

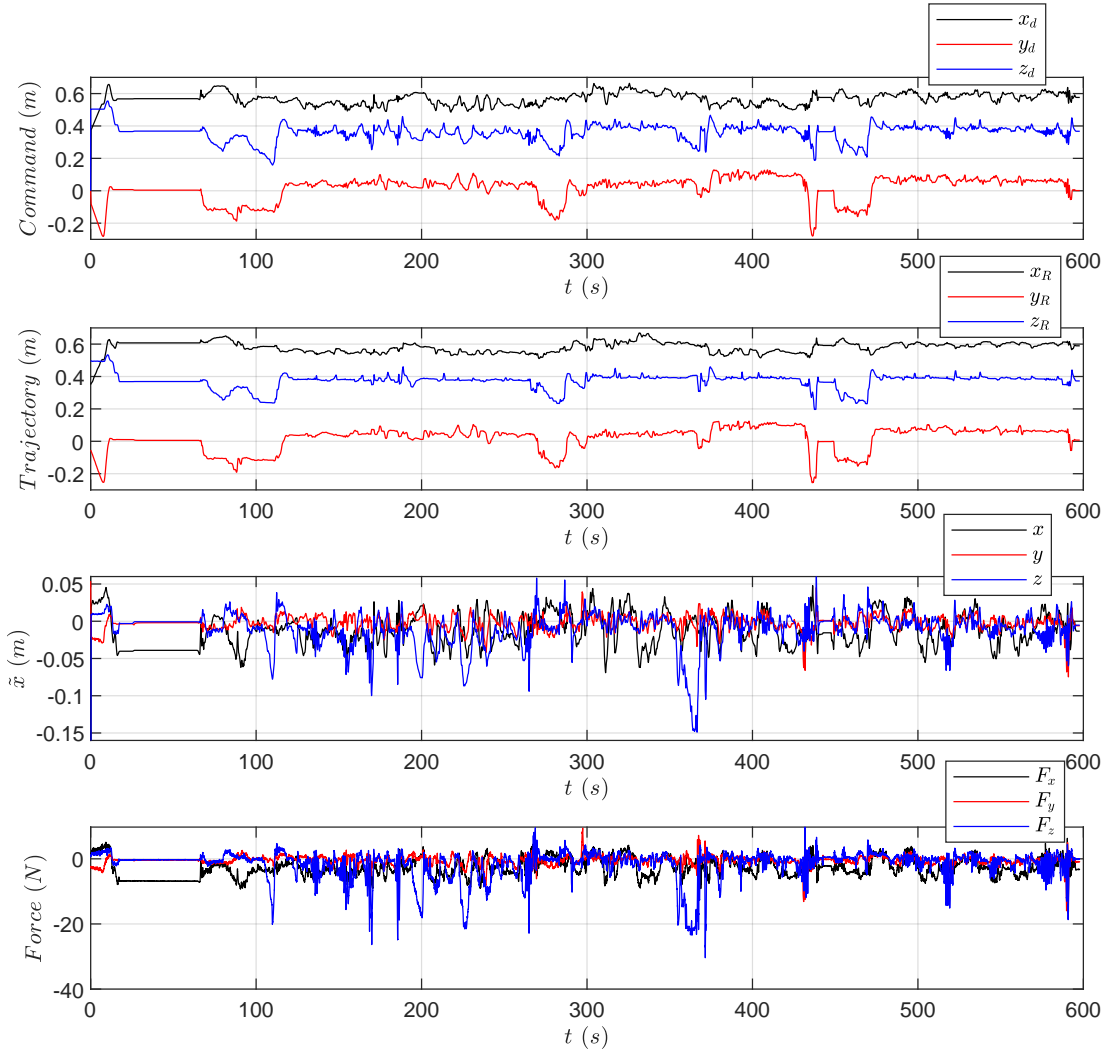


Fig. 3. The data indicate that the tracing accuracy is within the selected level ($\tilde{x}_b = 0.05$ m) whenever the system is not interacting with the environment. There are multiple peaks of the impacts that exceed the maximum value that can be generated by the controller, highlighting the dynamically challenging environment produced by these tasks. However, the controller can absorb the energy and maintain a safe and robust interaction.

the desired tracking accuracy is respected; however, there are four peaks where it is exceeded due to the interaction with the environment. Nevertheless, the system recovers as soon as the perturbation is removed. A tridimensional visualisation of the trajectory for the master and the replica during these experiment is shown in Fig. 8. We superimpose a periodic circle motion of 20 cm of diameter and with a period of 5 s centred in between the two obstacles. They prove that the superimposition of the teleoperation command to the autonomous trajectory is feasible and does not impact the robustness and safety of interaction of the proposed method, as highlighted in Fig. 6. However, this experiment also highlights a limited spatial awareness of the operator and its impact on dynamic three-dimensional tasks. The recorded video data indicate that this is partially associated with limited depth perception provided by the cameras; nevertheless, other factors are affecting it. For example, we have found that this is also related to the lack of haptic feedback beyond the end-effector, shown in Fig. 9 where a

cable can be observed mounted on the robot touching the obstacle without the operator noticing it.

IV. DISCUSSION & CONCLUSION

The experiment on haptic fine teleoperation combined with force manipulation highlights the capabilities of our method to address complex environmental dynamics. This architecture has a decoupled stability between the master and the replica controllers, and it does not rely on the projected dynamics. These two factors determine the method scalability due to its computational efficiency and its robustness to communication disruption, unstructured interaction, and singularities. Additionally, the updated architecture can constraint the motion power within the limits of the replica robot allowing more challenging manoeuvres that are not possible with our earlier implementation of the FIC in teleoperation [13], [14].

The first experiment validates that the proposed teleoperation method can be used to perform robust fine manipulation

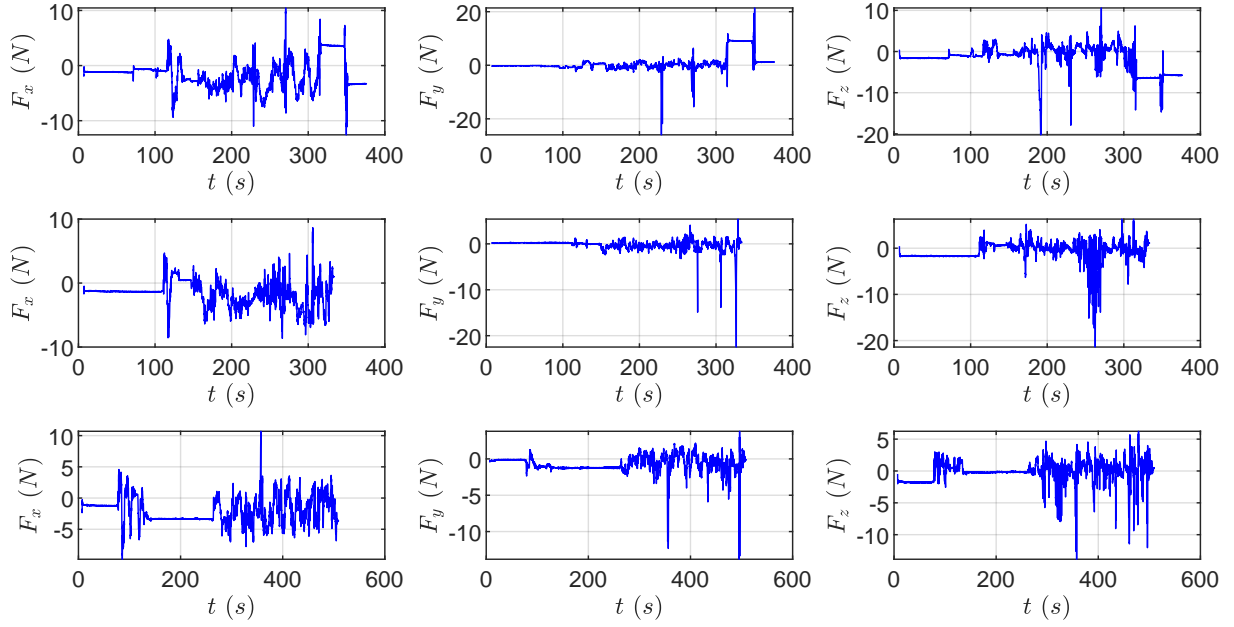


Fig. 4. Interaction forces recorded during the other three trials of the shape sorting cube. The second row from the top is the trial testing for the robustness to loss of communication between Master and Replica. After the disconnection occurred at about 280s, the replica continues to safely interact with the environment as in the other 2 experiments. The force signals show how the controller is intrinsically robust to multiple impulsive interactions with the environment.

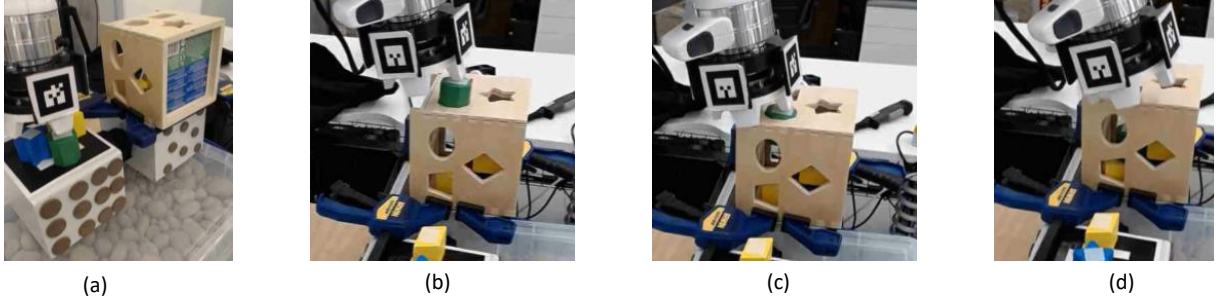


Fig. 5. Task's stages for the first experiment: (a) Object is picked up making a bound using the Velcro strap. (b) Object is aligned and inserted in the hole. (c) Object is locked against the hole sides. (d) User pulls the arm away breaking the bound with the object, which falls inside the cube.

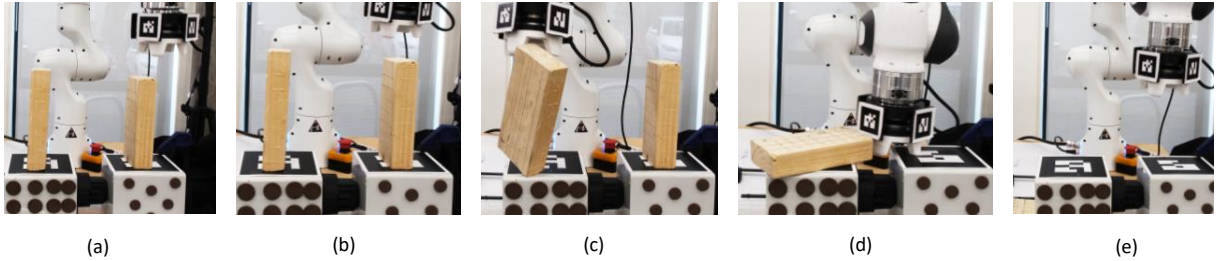


Fig. 6. Task's stages for the second experiment: (a) Robot approaches the first obstacle. (b) First obstacle is avoided. (c) Second obstacle is pushed out of the workspace. (d) Second obstacles is pushed out. (e) Robot continues executing the autonomous manipulation task until stopped.

during uncertain dynamic interaction with the environment. The second experiment shows how it is possible to superimpose the teleoperator action and autonomous trajectories. This operational method provides a hybrid method where we can exploit the benefit of autonomous manipulation without

renouncing the adaptability to environmental changes provided by the human operator. Manipulation algorithms can provide outstanding repeatability and account for the physical limitation of the robot in both kinematic and dynamic, but they might only partially capture complex environments.

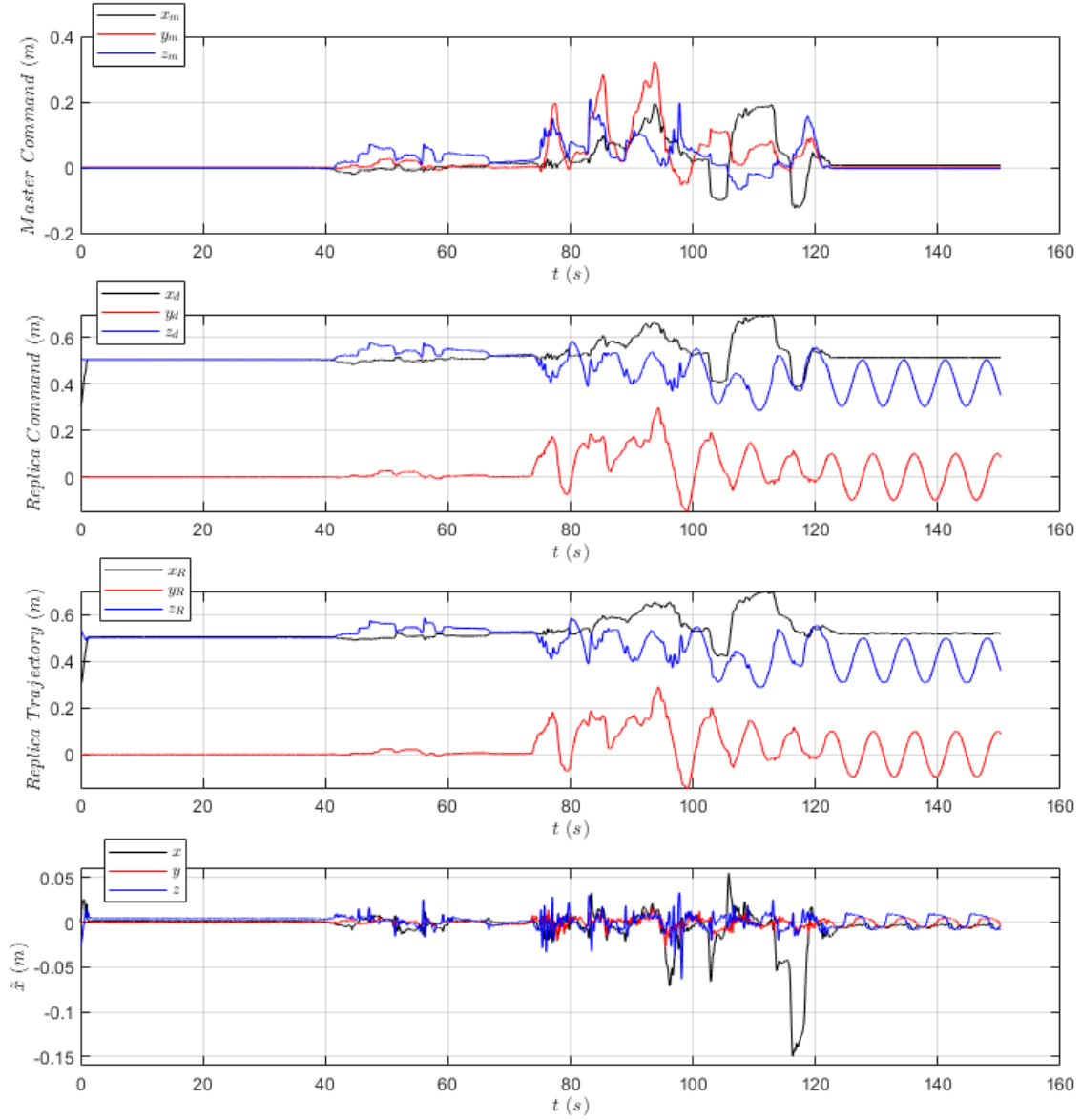


Fig. 7. The data show the tracking data from the superimposition experiments. The tracking error shows that the robot is mostly within the desired accuracy $\tilde{x}_b = 0.05$ m. There are four peaks that exceed the tracking accuracy when the robot is interacting with the environment.

Therefore, the human operator can be exploited to respond to the variable components of the task which are difficult to capture using model-based solutions, such as reacting unforeseen obstacles and interacting with unknown objects.

The proposed control architecture showed flexibility of interaction, and a multi-modal deployment capabilities with the possibility to seemingly switch between manipulation and teleoperation as well as superimposing the two modality in presence of communication delays. Nevertheless, our experiments also indicate a limited spatial awareness of the user, which seems to increase with the task's dynamism. The limited perception directly impact the operator's cognitive load [25], [26], which has to learn and adapt his strategies to the system. This should be improved in the future by

studying how to improve the embodiment of artificial arms.

REFERENCES

- [1] P. Schmaus, D. Leidner, T. Krüger, R. Bayer, B. Pleintinger, A. Schiele, and N. Y. Lii, "Knowledge driven orbit-to-ground teleoperation of a robot coworker," *IEEE Robotics and Automation Letters*, vol. 5, no. 1, pp. 143–150, 2019.
- [2] A. Toet, I. A. Kuling, B. N. Krom, and J. B. Van Erp, "Toward enhanced teleoperation through embodiment," *Frontiers in Robotics and AI*, vol. 7, p. 14, 2020.
- [3] L. Penco, B. Clément, V. Modugno, E. M. Hoffman, G. Nava, D. Pucci, N. G. Tsagarakis, J.-B. Mouret, and S. Ivaldi, "Robust real-time whole-body motion retargeting from human to humanoid," in *2018 IEEE-RAS 18th International Conference on Humanoid Robots (Humanoids)*. IEEE, 2018, pp. 425–432.
- [4] Z. Chen, F. Huang, W. Sun, J. Gu, and B. Yao, "Rbf-neural-network-based adaptive robust control for nonlinear bilateral teleoperation ma-

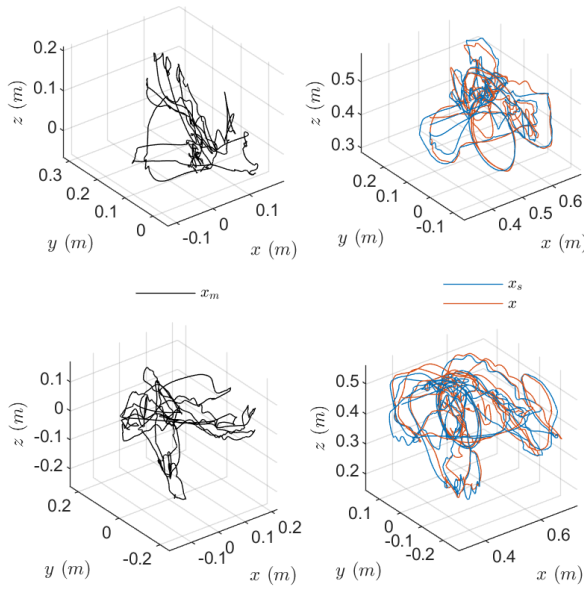


Fig. 8. On the top the first trail of the superimposition feasibility experiment. On the bottom the second trial. The effect of the user input (x_m) is evident in both the superimposed trajectories (x_s), and the measured end-effector trajectory. The undisturbed circular trajectory can be still be seen in both trials in the x_s and x in both cases.

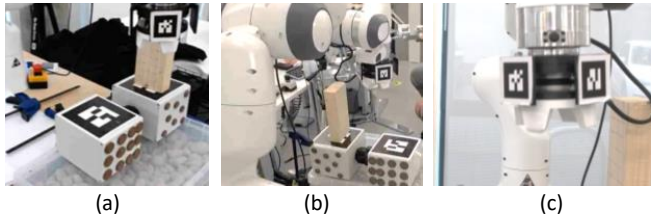


Fig. 9. This figure showcases the importance of providing the user with adequate special awareness during dynamics task, which is challenging when dealing with fixed camera placement. (a) and (b) are the two camera view provided to the user, which do not allow to detect the cable collision. (c) A third camera that allows to identify the collision.

nipulators with uncertainty and time delay,” *IEEE/ASME Transactions on Mechatronics*, vol. 25, no. 2, pp. 906–918, 2019.

- [5] J. I. Lipton, A. J. Fay, and D. Rus, “Baxter’s homunculus: Virtual reality spaces for teleoperation in manufacturing,” *IEEE Robotics and Automation Letters*, vol. 3, no. 1, pp. 179–186, 2017.
- [6] T. Hulin, M. Panzirsch, H. Singh, R. Balachandran, A. Coelho, A. Pereira, B. M. Weber, N. Bechtel, C. Riecke, B. Brunner, *et al.*, “Model-augmented haptic telemanipulation: Concept, retrospective overview and current use-cases,” *Frontiers in Robotics and AI*, vol. 8, p. 76, 2021.
- [7] M. Elobaid, Y. Hu, G. Romualdi, S. Dafarra, J. Babic, and D. Pucci, “Telepresence and teleoperation for walking humanoid robots,” in *Proceedings of SAI Intelligent Systems Conference*. Springer, 2019, pp. 1106–1121.
- [8] N. Feizi, M. Tavakoli, R. V. Patel, and S. F. Atashzar, “Robotics and ai for teleoperation, tele-assessment, and tele-training for surgery in the era of covid-19: existing challenges, and future vision,” *Frontiers in Robotics and AI*, vol. 8, 2021.

- [9] P. Beckerle, C. Castellini, and B. Lenggenhager, “Robotic interfaces for cognitive psychology and embodiment research: a research roadmap,” *Wiley Interdisciplinary Reviews: Cognitive Science*, vol. 10, no. 2, p. e1486, 2019.
- [10] Z. Chen, F. Huang, C. Yang, and B. Yao, “Adaptive fuzzy backstepping control for stable nonlinear bilateral teleoperation manipulators with enhanced transparency performance,” *IEEE transactions on industrial electronics*, vol. 67, no. 1, pp. 746–756, 2019.
- [11] H. Su, C. Yang, H. Mdeihly, A. Rizzo, G. Ferrigno, and E. De Momi, “Neural network enhanced robot tool identification and calibration for bilateral teleoperation,” *IEEE Access*, vol. 7, pp. 122 041–122 051, 2019.
- [12] H. Su, W. Qi, C. Yang, J. Sandoval, G. Ferrigno, and E. De Momi, “Deep neural network approach in robot tool dynamics identification for bilateral teleoperation,” *IEEE Robotics and Automation Letters*, vol. 5, no. 2, pp. 2943–2949, 2020.
- [13] K. K. Babarhamati, C. Tiseo, Q. Rouxel, Z. Li, and M. Mistry, “Robust high-transparency haptic exploration for dexterous telemanipulation,” in *Proc. IEEE International Conference on Robotics and Automation (ICRA)*, 2021.
- [14] —, “Robust and dexterous dual-arm tele-cooperation using fractal impedance control,” *arXiv preprint arXiv:2108.04567*, 2021.
- [15] K. K. Babarhamati, C. Tiseo, J. Smith, H. C. Lin, M. S. Erden, and M. Mistry, “Fractal impedance for passive controllers,” *arXiv preprint arXiv:1911.04788*, 2019.
- [16] F. Ferraguti, N. Preda, A. Manurung, M. Bonfe, O. Lamercy, R. Gassert, R. Muradore, P. Fiorini, and C. Secchi, “An energy tank-based interactive control architecture for autonomous and teleoperated robotic surgery,” *IEEE Transactions on Robotics*, vol. 31, no. 5, pp. 1073–1088, 2015.
- [17] M. Minelli, F. Ferraguti, N. Piccinelli, R. Muradore, and C. Secchi, “An energy-shared two-layer approach for multi-master-multi-slave bilateral teleoperation systems,” in *2019 International Conference on Robotics and Automation (ICRA)*. IEEE, 2019, pp. 423–429.
- [18] C. Tiseo, W. Merkt, K. K. Babarhamati, W. Wolfslag, S. Vijayakumar, and M. Mistry, “Bio-mimetic adaptive force/position control using fractal impedance,” in *2020 8th IEEE RAS/EMBS International Conference for Biomedical Robotics and Biomechanics (BioRob)*, 2020, pp. 1180–1187.
- [19] C. Tiseo, Q. Rouxel, Z. Li, and M. Mistry, “Robust impedance control for dexterous interaction using fractal impedance controller with ik-optimisation,” in *Proc. IEEE International Conference on Robotics and Automation (ICRA)*, 2022 (In Press).
- [20] C. Tiseo, W. Merkt, K. K. Babarhamati, W. Wolfslag, I. Havoutis, S. Vijayakumar, and M. Mistry, “Haptic: An adaptive force/position controller for safe environment interaction in articulated systems,” *IEEE Transactions on Neural Systems and Rehabilitation Engineering*, pp. 1–1, 2021.
- [21] C. Tiseo, S. R. Charitos, and M. Mistry, “Harmonic passive motion paradigm,” *bioRxiv*, 2021. [Online]. Available: <https://www.biorxiv.org/content/early/2021/07/08/2021.07.06.451400>
- [22] C. Tiseo, V. Ivan, W. Merkt, I. Havoutis, M. Mistry, and S. Vijayakumar, “A passive navigation planning algorithm for collision-free control of mobile robots,” in *Proc. IEEE International Conference on Robotics and Automation (ICRA)*, 2021.
- [23] C. Tiseo, S. R. Charitos, and M. Mistry, “Theoretical evidence supporting harmonic reaching trajectories,” in *2021 10th International IEEE/EMBS Conference on Neural Engineering (NER)*. IEEE, 2021.
- [24] C. Tiseo, Q. Rouxel, Z. Li, and M. Mistry, “Video of the experiments,” https://youtu.be/xC-IrZh_FbY.
- [25] L. Aymerich-Franch, D. Petit, G. Ganesh, and A. Kheddar, “Non-human looking robot arms induce illusion of embodiment,” *International Journal of Social Robotics*, vol. 9, no. 4, pp. 479–490, 2017.
- [26] T. R. Makin, F. de Vignemont, and A. A. Faisal, “Neurocognitive barriers to the embodiment of technology,” *Nature Biomedical Engineering*, vol. 1, no. 1, pp. 1–3, 2017.